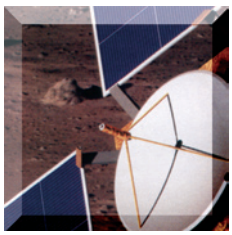

Near Earth Asteroid Rendezvous: The Science of Discovery

Deborah L. Domingue and Andrew F. Cheng

The Near Earth Asteroid Rendezvous (NEAR) mission, the first in NASA's Discovery Program, launched on 17 February 1996. Almost 4 years later (14 February 2000) the NEAR spacecraft (NEAR Shoemaker) began the first orbital study of an asteroid, the near-Earth object 433 Eros. NEAR Shoemaker completed its mission on 12 February 2001 by landing on the asteroid and acquiring data from its surface. In addition to its detailed study of the S-type asteroid 433 Eros, NEAR Shoemaker also performed the first flyby measurements of a C-type asteroid, 253 Mathilde, en route to its target destination. This successful mission has provided a new wealth of discoveries in the field of asteroid science and has led to new lines of thought about asteroids, their formation, and their evolution.

INTRODUCTION

The Near Earth Asteroid Rendezvous (NEAR) mission was a science mission of many historical firsts. Launched on 17 February 1996, it was the first in NASA's new Discovery Program. Its science investigation began with the first flyby of a C-type asteroid, 253 Mathilde, on 27 June 1997. Subsequently it flew by S-type asteroid 433 Eros, its primary target, on 13 December 1998. On 14 February 2000, almost 4 years after launch, it made history by being the first spacecraft to orbit an asteroid when it entered orbit around Eros. The spacecraft was then renamed NEAR Shoemaker in honor of the late Eugene M. Shoemaker (1928–1997), a pioneer in asteroid and crater science. NEAR accomplished another historical first when on 12 February 2001 it gently touched down on Eros' surface (Fig. 1) and returned scientific measurements from the asteroid's surface for an additional 10 days.[1,2]

The NEAR Shoemaker spacecraft carried onboard a six-instrument scientific payload in addition to a radio science investigation using the spacecraft telecommunications system. The instruments included three spectrometers (near-infrared, X-ray, and gamma-ray), a multispectral imager, a laser rangefinder, and a magnetometer. Detailed descriptions of the spacecraft's performance and the science instruments are given in articles by Santo and Gold elsewhere in this issue, in the *Journal of Astronautical Sciences* 43(4), and in articles included in both the *Technical Digest* 19(2) and *Advances in Astronomical Sciences* 109. Other articles in this issue also describe the details of the mission design (Dunham et al.), mission operations (Holdridge), spacecraft navigation (Williams), science operations (Holland), and science planning (Heyler and Harch). The following is a discussion of the scientific

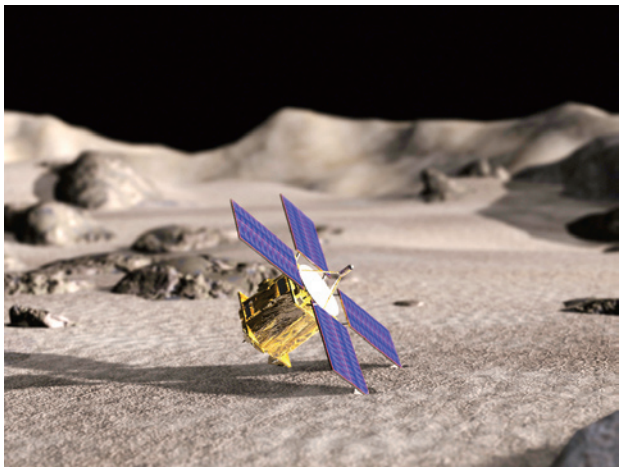

Figure 1. Artist's rendition of the NEAR Shoemaker spacecraft on the surface of Eros after its historic landing.

results obtained during the Mathilde flyby and the rendezvous with Eros. As with most successful exploration missions, NEAR answered the questions it was designed to investigate and tantalized us with observations that have led to new directions of inquiry.

SCIENCE BACKGROUND

Between the orbits of Mars and Jupiter reside the main-belt asteroids, the largest known population of such bodies. Another population, the near-Earth asteroids, have orbits that come within 1.3 AU of the Sun and are believed to originate from the main belt. The orbits of these former main-belt asteroids have evolved on 100-million-year timescales owing to collisions, the Yarkovsky effect (reaction force from anisotropic emission of thermal radiation), and gravitational interactions with the planets[3] to their present locations. Because of their evolutional link to the main belt, near-Earth asteroids represent a broad sample of the main-belt asteroid population.

Prior to the mission, the NEAR Science Working Group[4] identified some of the key gaps in our understanding about asteroids. The questions they formulated fell into two basic categories: (1) how did small bodies in the solar system form and evolve, and (2) how can asteroids be linked to the collection of asteroid samples (known as meteorites) we currently have on Earth? Understanding the formation and evolution of asteroids, which are some of the most primitive bodies in the solar system, increases our knowledge of the origin and evolution of planets within the solar system as well as the environment of the early solar system. Establishing a correlation between the meteorite classes and asteroid types also increases our understanding of the origin and evolution of the solar system by allowing us to compare the "hand samples" we have in meteorites with their source regions in the solar system. From studies of the mineralogy and petrology of the meteorites we gain an insight into which processes were at work as well as when and where they occurred in the early solar system.

Knowledge and information on the nature of asteroids prior to the NEAR mission came from three sources: (1) Earth-based remote sensing, (2) spacecraft flybys (Galileo flybys of two main-belt S-type asteroids, 951 Gaspra and 243 Ida), and (3) laboratory analysis of meteorites. To comprehend the formation and evolution of small solar system bodies such as asteroids, we need information about their composition (both mineral and elemental), internal structure, and surface processes. Earth-based remote sensing has yielded a wealth of information on the global mineral composition of various asteroid types from spectral measurements. Actually, an asteroid's type classification is based on spectral signature. Disk-resolved spectral information, however, had been limited to color measurements obtained by the Hubble Space Telescope[5–13] and the Galileo spacecraft. Before the NEAR mission, no direct measurement of mineral and elemental compositional information for asteroids had been available. Such knowledge is needed to determine if an asteroid has undergone melting and differentiation (gravitationally driven partition of materials), and to what degree it has been melted and/or differentiated. This information, coupled with its size and an understanding of its internal structure, can help establish whether the asteroid is a shard from a larger object or an agglomeration of gravitationally bound rubble.

An asteroid's internal structure is largely determined by its collisional history during its evolution. An asteroid that has been battered into an agglomeration of much smaller components bound by gravity (a rubble pile) has undergone a very different collisional history from one that is an intact collisional fragment from a larger parent body (a collisional shard). A collisional shard would be a globally consolidated body with appreciable shear and/or tensile strength, for which self-gravitation would be relatively unimportant. For example, Gaspra's faceted shape and the presence of grooves on its surface hint at such a structure.[14] However, an alternative picture for asteroids the size of Eros is that they were thoroughly broken up without being dispersed (or possibly re-accreted), so they would now be rubble piles (e.g., Refs. 15 and 16). Some small asteroids rotate so rapidly that they must be monolithic (e.g., Ref. 17), but no asteroids larger than 0.2 km have been found with rotation periods shorter than 2 h, suggesting that most of these larger bodies are rubble piles.[18]

The majority of meteorites are believed to be collisional fragments of asteroids (a few come from the Moon and Mars). The proposed links between asteroids and meteorites are highly controversial, and firm correlations between meteorite types and asteroid types have been

difficult to establish.[19] For example, ordinary chondrite and anchondrite meteorites are both proposed candidates for S-type asteroids, the most common asteroid type in the inner part of the main belt. Ordinary chondrites (the most common meteorite type) are primitive and relatively unprocessed, whereas achondrites represent bodies that have undergone thermal processing. Although some S-type asteroids appear to be fragments of bodies that underwent substantial melting and differentiation (e.g., achondrites), others (e.g., ordinary chondrites) appear to consist of primitive materials that underwent little or no melting. Since the S-type asteroids are the objects most likely to have preserved characteristics of the solid material from which the inner planets accreted, establishing their link to the meteorite types will enable us to understand the early solar system environment from which the inner planets evolved.

Attempts have been made to use spectral observations to link asteroid and meteorite types. Few definitive spectral analogs for ordinary chondrites have been found among the asteroids. Space-weathering processes such as micrometeorite bombardment and radiation processing may suitably alter spectral properties of optical surfaces on asteroids[20,21] so that ordinary chondrite materials on asteroids are not recognized spectrally.

SCIENTIFIC RESULTS

The Galileo spacecraft flybys of Gaspra and Ida provided the first high-resolution images of asteroids. These images revealed complex surfaces covered by craters, fractures, grooves, and subtle color variations.[22,23] Galileo also discovered Ida's satellite Dactyl.[24] The Galileo flyby measurements demonstrated the wealth of information that can be obtained about asteroids through spacecraft encounters. NEAR's scientific findings, presented here, reemphasize the wealth of knowledge gained through spacecraft encounters by providing us with information on two very different asteroids.

Mathilde

In October 1991 and September 1993 the Galileo spacecraft flew by the S-type asteroids 951 Gaspra and 243 Ida, respectively. NEAR Shoemaker's encounter with 253 Mathilde in July 1997 was the first spacecraft encounter with a C-type asteroid, the most common asteroid type in the central portion of the main belt. C-type asteroids are inferred to have a carbonaceous composition based on their spectral similarity to carbonaceous chondrite meteorites. The nature and origins of the dark, primitive asteroid types (like C-types) and their relationships to the comets and the dark objects in the satellite systems of the outer planets are among the most important unresolved issues in solar system exploration. NEAR's observations of an example of such an object have provided insight that was previously unattainable.

NEAR Shoemaker acquired more than 500 images of Mathilde[25] and obtained the first direct mass determination (1.03×10^{20} g) of an asteroid[26] from radio tracking of the spacecraft. Only one face of Mathilde was imaged during the 25-min flyby. Its volume (78,000 km^3) was estimated based on the shape of the imaged hemisphere, as derived from limb fits and stereogrammetry,[25] and on ground-based light-curve observations[27] to constrain the unimaged portion. The measured mass and estimated volume imply a density of 1.3 ± 0.3 g cm^{-3}. Given the evidence that Mathilde's bulk composition is similar to that of carbonaceous chondrite meteorites,[28,29] the inferred density was unexpectedly low, half that of carbonaceous chondrite meteorites. This implies a high internal porosity, or volume fraction of void space, on the order of 40 to 60%.[30] This high porosity has direct implications and constraints for the surface geology and internal structure of Mathilde.

The images taken during the flyby (Fig. 2) show that Mathilde's surface is heavily cratered; at least four giant craters have diameters that are comparable to the asteroid's mean radius (26.5 km). The magnitude of the impacts required to create craters of this size, if the crater formation process were controlled by gravity, is believed to be close to that needed to completely disrupt Mathilde. So why didn't Mathilde break apart during any of the impact events that created these craters? Part of the answer lies in Mathilde's high porosity.[30–32] Laboratory experiments on cratering in highly porous targets[33] have demonstrated that crater formation is governed by compaction of the target material rather than by fragmentation and excavation. Cratering processes governed by material properties (like porosity) produce craters with fresh morphologies (steep walls and crisp rims) and with little ejecta (e.g., Refs. 34–37). The

Figure 2. Mosaic of asteroid 253 Mathilde constructed from four images taken during NEAR Shoemaker's flyby in July 1997.

relatively fresh morphologies and absence of obscuring ejecta blankets associated with Mathilde's large craters support the notion that Mathilde's porosity plays an important role in the cratering process.[32,33]

Another consideration is that roughly half of all impacts are oblique. Oblique impacts are less likely to disrupt a target since they generate lower peak pressure and lower peak strain rates. If Mathilde's oblique impacts and porosity are taken into account, the probability of making a giant crater is 2.1 to 2.6 times more than the probability of disruption.[38] These results may explain not only how Mathilde survived so many giant impacts, but also how a giant crater can be emplaced practically adjacent to another without disrupting it.

The relatively lower resolution of the Mathilde images compared to the images obtained at Gaspra, Ida, and Eros restricts the analysis of the smaller-scale surface morphology. The images show that craters of all degradation states are present, and the areal density of craters with up to a 5-km diameter approaches saturation equilibrium, with a size distribution similar to that observed on Ida.[31] At the current resolution the images do not show any evidence for layering on the interior of the crater walls; however, there is evidence for possible mass-wasting chutes and slides in the interior of the large crater Karoo as well as a slump of material on the floor of the 7-km crater Lublin.[32]

Mathilde's low density and high porosity are consistent with a rubble pile structure. Nevertheless, the nature and distribution of voids within the interior is not well constrained. Nor is the history of Mathilde's porosity well known. Did this asteroid originally accrete as a porous structure and survive as such to the present, or, alternatively, is Mathilde an agglomerate of larger fragments, subsequently accreted to form this asteroid? If the latter is true, Mathilde may have been thoroughly disrupted by impacts but not dispersed; thus macroscopic voids would be expected, possibly in addition to microscopic porosity.

Color images show Mathilde to be remarkably uniform. The NEAR observations revealed no evidence for any regional albedo or spectral variations, implying a homogeneous composition. The measured geometric albedo (0.043 ± 0.005) is consistent with telescopic observations[39] (improved calibration is given in Ref. 40). The implied homogeneity in composition is another constraint on Mathilde's structure.

The NEAR imaging observations provide additional clues to the nature of Mathilde's internal structure. If Mathilde accreted fragments of diverse parent bodies, these must have had remarkably uniform albedos and colors, or else the fragments must be smaller than about 500 m. Evidence for structure has been reported from images; there are polygonal craters, a 20-km-long marking interpreted as a scarp, and a sinuous linear feature that may be an exposed layer.[32] Mathilde's high porosity is key to understanding its collisional history, but its structural features, such as the aforementioned scarp and its polygonal craters, indicate that it is not completely strengthless and that at least one of its structural components appears coherent over a few tens of kilometers.

Eros

NEAR Shoemaker encountered Eros (Fig. 3) twice, first with a flyby in December 1998 and finally with an orbital mission from 2000 to 2001. The flyby observations greatly facilitated the Eros orbital mission and allowed an earlier start to the low-altitude phase of the primary mission. The flyby and orbital observations yielded values of the mass and density of $6.687 \pm 0.003 \times 1015$ kg and 2670 ± 30 kg m^{-3}, respectively.[41] The size and rotation pole of Eros were found to be consistent with previous ground-based determinations.[42,43]

NEAR Shoemaker's instruments provided measurements indicating that Eros is a consolidated body, not a loosely bound agglomeration of smaller component bodies or a rubble pile.[30,44,45] The measured gravity field is consistent with a uniform density object of the same shape.[41] Comparisons of Eros' measured density with laboratory measurements of the density of ordinary chondrite meteorites[46] estimate Eros' bulk porosity to be 21 to 33%. This implies that even though the asteroid's mass is uniformly distributed, it is significantly porous and/or fractured, but not to as large an extent as Mathilde. The size scale of this porosity (microporosity on the scale of grains or macroporosity on the

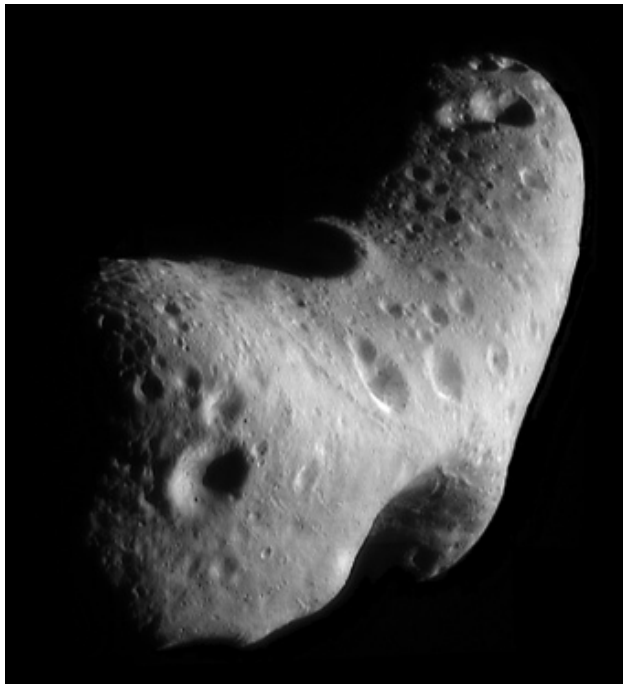

Figure 3. Mosaic of the northern hemisphere of Eros, acquired from a 200-km orbit.

scale of structural elements) is not constrained by the gravity or density measurements, but is commensurate with a heavily fractured consolidated body rather than a rubble pile.[47,48] There is a less than 1% center of mass offset from the center of figure,[49,50] which is consistent with an underdense regolith (unconsolidated dust) layer of up to a 100-m depth.[45]

Additional evidence that Eros is a consolidated body is found in the NEAR images. These show linear structural features—a variety of ridges, grooves, and chains of pits or craters[44] that display regionally coherent alignments over several kilometers (Fig. 4). A handful of large-scale structures (Fig. 5) have been identified, showing evidence for a global structural fabric. These include Rahe Dorsum, Calisto Fossae (a long ridge system at 25°S, 150°–170°W), and a set of grooves at 50°–60°S. Suggested origins for Eros' global structural fabric include compositional layering, preexisting fractures, and a metamorphic fabric.[48] The spectral homogeneity observed on Eros[51,52] supports an origin due to fracturing or thermal- or pressure-related metamorphosis within Eros' parent body.[48] Evidence for structural strength is also found from crater morphologies: many craters smaller than 1 km appear to be jointed and/or structurally controlled,[53] although larger craters (such as Psyche) are bowl-shaped. Additional evidence for a consolidated body is found in the presence of steep slopes (Fig. 6), which are well above expected angles of repose.[45] Taken together, the gravity field measurements, linear structural features, tectonic features such as Rahe Dorsum, jointed craters, and indications of internal structural coherence all suggest that Eros is a collisional fragment from a larger parent body, or a so-called "collisional shard."

Examining Eros' cratering record tells us a great deal about its geologic history. Figure 7 compares the

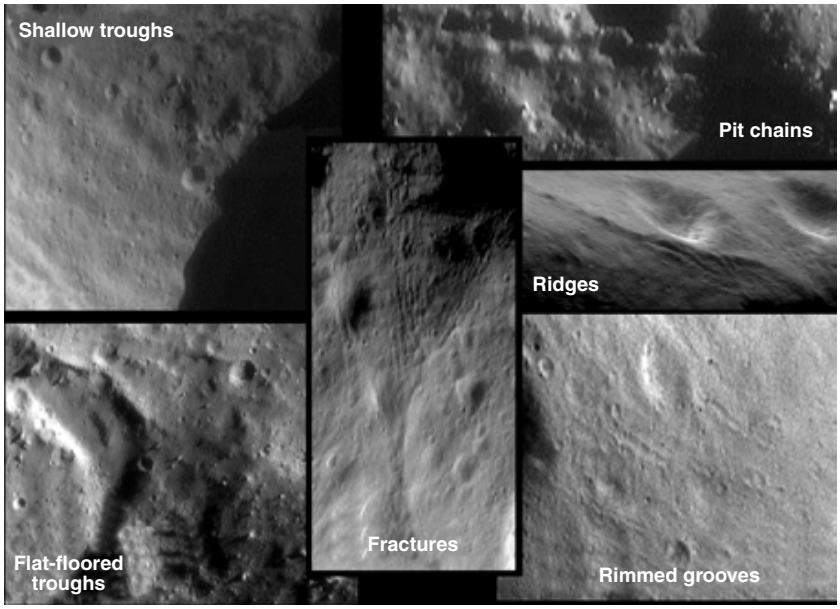

Figure 4. Images from the NEAR Multispectral Imager camera showing the variety of structural features found on the surface of Eros that are indicative of a coherent, consolidated substrate.

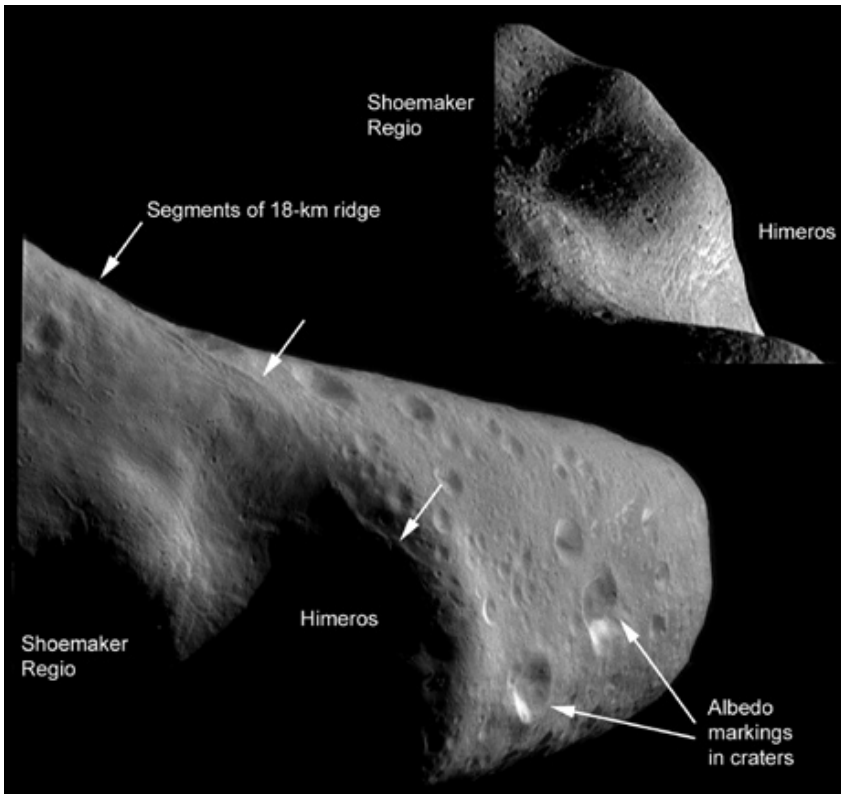

Figure 5. Eros from a 200-km orbit. At lower left and center, the saddle-shaped depression Himeros and the boulder-rich depression Shoemaker Regio are marked (these regions are in shadow). A portion of the 18-km-long ridge (Rahe Dorsum), which continues over the horizon, is marked with the shorter arrows. The density of craters larger than 500 m is much greater outside of Himeros and Shoemaker Regio. Systems of crosscutting grooves are seen in Himeros. Many crater walls exhibit bright and dark albedo markings. The Sun is to the right. At the upper right is another view of Himeros and Shoemaker Regio.

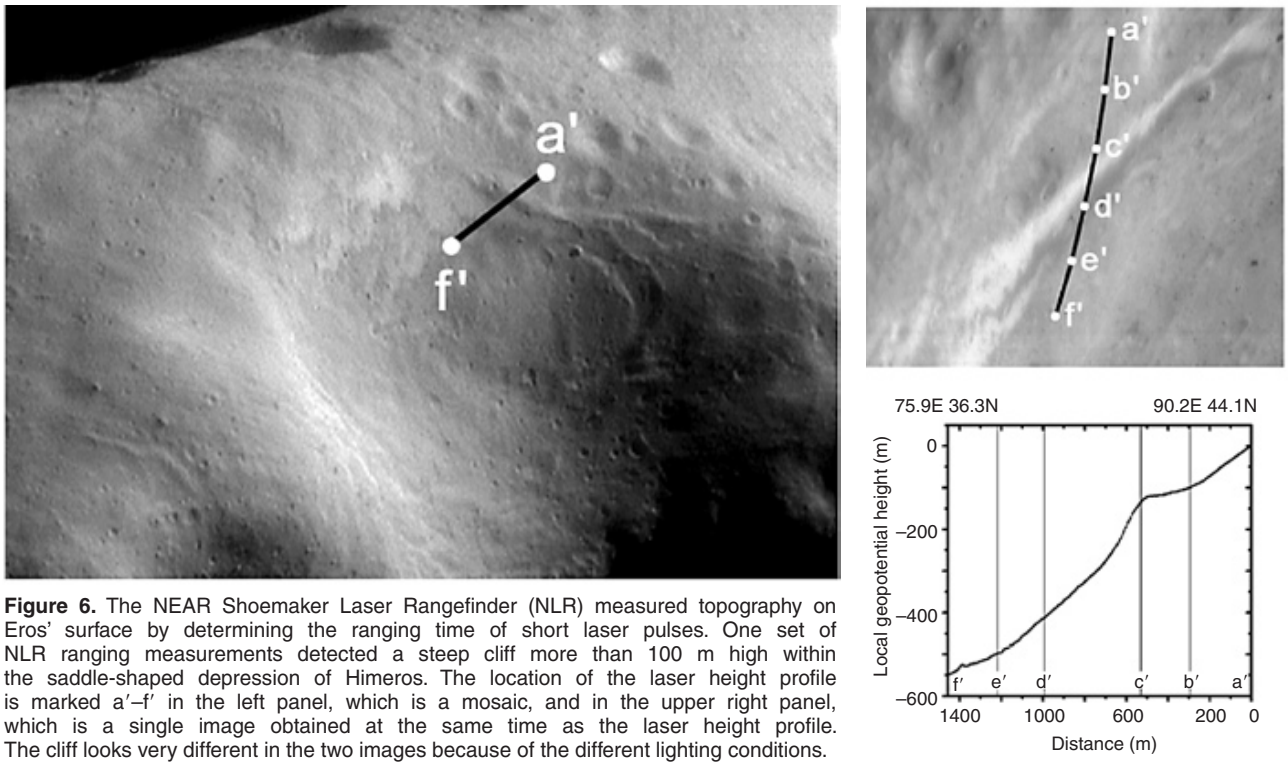

Figure 6. The NEAR Shoemaker Laser Rangefinder (NLR) measured topography on Eros' surface by determining the ranging time of short laser pulses. One set of NLR ranging measurements detected a steep cliff more than 100 m high within the saddle-shaped depression of Himeros. The location of the laser height profile is marked a′–f′ in the left panel, which is a mosaic, and in the upper right panel, which is a single image obtained at the same time as the laser height profile. The cliff looks very different in the two images because of the different lighting conditions.

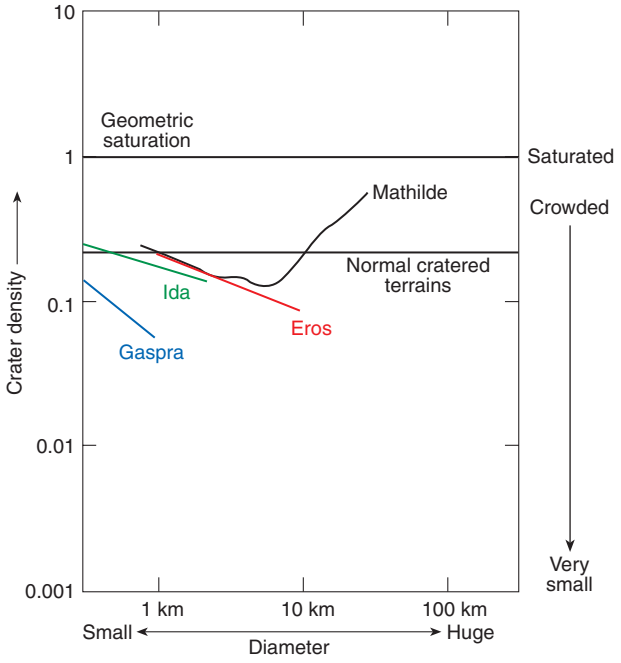

Figure 7. This graph compares impact crater populations on the various asteroids visited by spacecraft. The density of the craters increases from bottom to top of the graph. The line labeled "geometic saturation" represents the crater density where craters would totally crowd the surface. A distinction made between asteroids is whether large or small craters dominate the surface coverage. A line sloping to the upper right indicates large craters dominating the surface coverage, whereas a line sloping to the upper left indicates small craters dominating the surface coverage. This plot demonstrates that Eros has similar numbers of small craters as Mathilde and Ida but lacks the number of large craters observed on Mathilde. The low number of craters observed on Gaspra compared to Eros, Ida, and Mathilde indicates that Eros' surface is younger than the others.

size density of craters found on Eros to other asteroids visited by spacecraft. In contrast to the large craters seen on Mathilde, the morphology of the three largest impacts on Eros (Himeros at ≈9.0 km, Shoemaker at 7.6 km, and Psyche at 5.3 km) displays shapes, depth/diameter ratios, and rims (for Shoemaker and Psyche) that are consistent with gravity controlled impact excavation.[54] Most of the surface is old and close to equilibrium saturation, with craters larger than 200 m in diameter.[44,55] However, Eros' surface is deficient in craters smaller than 200 m in diameter.[48,55] Crater densities also vary across Eros' surface.

The NEAR images show evidence for globally distributed crater ejecta in the form of blocks and boulders. These ejecta are observed ubiquitously over Eros' surface. Mapping of the larger blocks reveals a concentration at low latitudes, with nearly half the mapped volume of blocks residing within the Shoemaker impact crater.[50] Most of the blocks and boulders outside Shoemaker display a distribution that is commensurate with a probable origin from the impact that created the crater.[50] The lack of blocks and boulders associated with ejecta from Psyche and Selene implies that the ejecta from these older craters has been buried or eroded, or may not have initially contained the number of blocks produced by the Shoemaker impact.[48,50] The blocks have shapes ranging from angular to rounded and clod-like with varying degrees of degradation.[50,56] The density of small craters (under 100 m) is markedly depleted on Eros compared to the Moon, but the density of boulders is markedly enhanced.

Polarimetric and thermal studies[57–59] have supported the presence of a fine-grained regolith layer on Eros. The surface morphology seen in the NEAR images verified the presence of a complex regolith (Fig. 8).[56] This is inferred from the dearth of small craters (<100 m), the profusion of blocks and boulders in various states of burial, and evidence for burial of small craters and mass wasting.[54,60] The regolith's depth is estimated to be on the order of tens of meters based on measurements of filled craters and benches,[61] the slump morphology observed in Himeros,[48] and the global groove morphology.[53] Craters on Eros are typically shallower than lunar craters of the same diameter, consistent with a regolith depth ranging from tens of meters to less than 100 m close to the largest impact craters.[61]

Eros' regolith has been significantly modified and redistributed by gravity-driven slope processes. Examples include the high albedo features seen on sloped crater walls (Fig. 9) and the burial of craters on slopes and in depressions. The high albedo features occur approximately parallel to the slope contours[54] and are typically 1.5 times brighter than their surroundings. They occur preferentially where slopes exceed 25°.[62,63] These features' higher albedo and subtle color differences from their surroundings are consistent with effects of space weathering due to exposure of fresher subsurface material. However, the color variations associated with these high albedo spots are nearly 10 times weaker than those associated with high-albedo exposures of fresh materials on the Moon. This difference is best explained by differences in the small-scale physical effects of space weathering on mineral grains between the Moon and Eros.[62]

The slopes of Himeros exhibit the most prominent landforms indicative of mass wasting, including dark markings extending 2 km down the eastern slopes.[54] Hummocky topography indicates landslide-like movement of perhaps tens of meters of debris down the northeast side of Himeros, as well as slumps tens of meters thick on the crater's western slopes.[48]

An unexpected finding at Eros was the discovery of extremely level, ponded deposits.[56,64–66] The ponds are characterized by smooth, sharply bounded surfaces in gravitational lows (Fig. 10). Their morphology is consistent with emplacement of material with no shear strength, so they act like a fluid and "pond" with an equipotential surface.[48] Images of many of these deposits show the presence of steep-walled grooves, impact craters, and superposed blocks, implying that subsequent to their formation, compaction and cohesion has occurred to create non-zero shear strength.[48] They have color properties distinct from the rest of Eros' surface, suggesting that the ponds are concentrations of fine-grained material.[66] Their color and spectral properties are consistent with a lower exposure to space weathering processes than the remainder of Eros' surface.[66] Processes such as electrostatic sedimentation and seismic shaking from impacts have been discussed as possible means to concentrate fine particulates to form these ponded deposits.

Figure 8. Evidence for a fragmental regolith cover on Eros includes the presence of blocks. The relatively large blocks in the lower left corner are ≈90 m across. They are surrounded by bright debris aprons, which are evidence for erosion. Many craters appear infilled. The bright albedo feature in the shallow crater at the top may have formed when dark material slid downslope, exposing bright material.

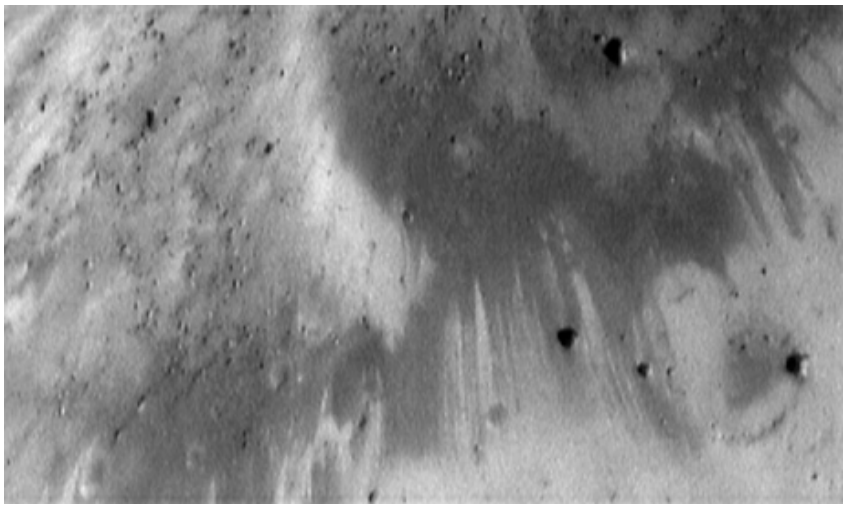

Figure 9. This image shows the interior wall of a large crater taken from an orbital altitude of 35 km. Like many steep slopes on Eros, this area is mottled with downward-oriented brightness streaks. The streaks are thought to be exposed subsurface material that has not been altered by space weathering processes. The whole scene is about 0.8 km across.

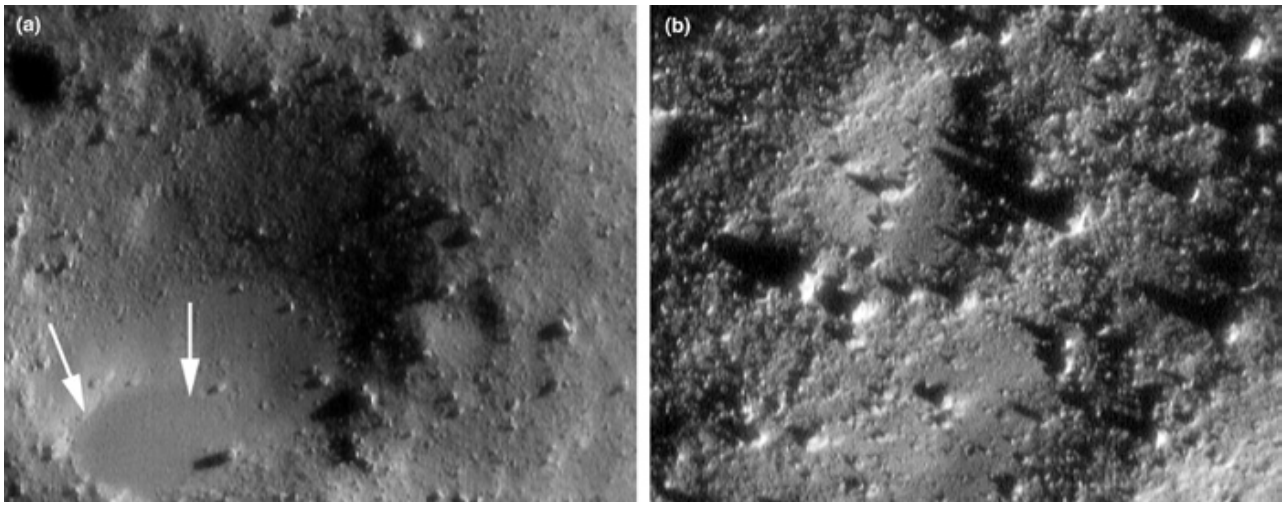

Figure 10. Eros close-up. (a) Arrows indicate a pond within a degraded crater; this frame is about 250 m across. (b) This frame is about 150 m across and illustrates the high density of boulders and the paucity of small, fresh craters.

NEAR Shoemaker carried three spectrographs to measure the elemental and mineral composition of Eros: the bulk elemental composition was measured independently by the X-Ray Spectrometer (XRS)[52] and the Gamma-Ray Spectrometer (GRS),[67] while the surface mineral composition was measured by the Near-Infrared Spectrometer (NIS).[51]

The orbital XRS data showed Ca, Al, Mg, Fe, and Si abundances consistent with ordinary chondrite and certain primitive achondrite meteorite compositions.[52] One unexpected finding from these measurements was the depletion of sulfur compared to abundances measured in chondritic meteorites. The XRS measures to a depth of only a few tens of microns. Thus it is unknown if the sulfur depletion is a surface effect or a bulk Eros phenomenon.[52] A bulk depletion would imply an association with primitive achondrite meteorites for Eros.[52] No evidence for spatial heterogeneity in elemental composition was seen by the XRS.

The GRS observations had lower signal levels than predicted, and the highest precision elemental abundance ratios were measured from the landing site (Fig. 11), a pond on the southeast border of Himeros.[67] The GRS surface data (Fig. 12) showed the Mg/Si and Si/O ratios and the abundance of K to be consistent with chondritic meteorite values, but found Fe/Si and Fe/O to be lower than chondritic.[68] The GRS data are sensitive to tens of centimeters depth, so this measurement pertains specifically to a volume on the order of a cubic meter of Eros. It is unknown from the GRS data alone whether the Fe depletion is a global compositional property or a property of the ponds. Images from the

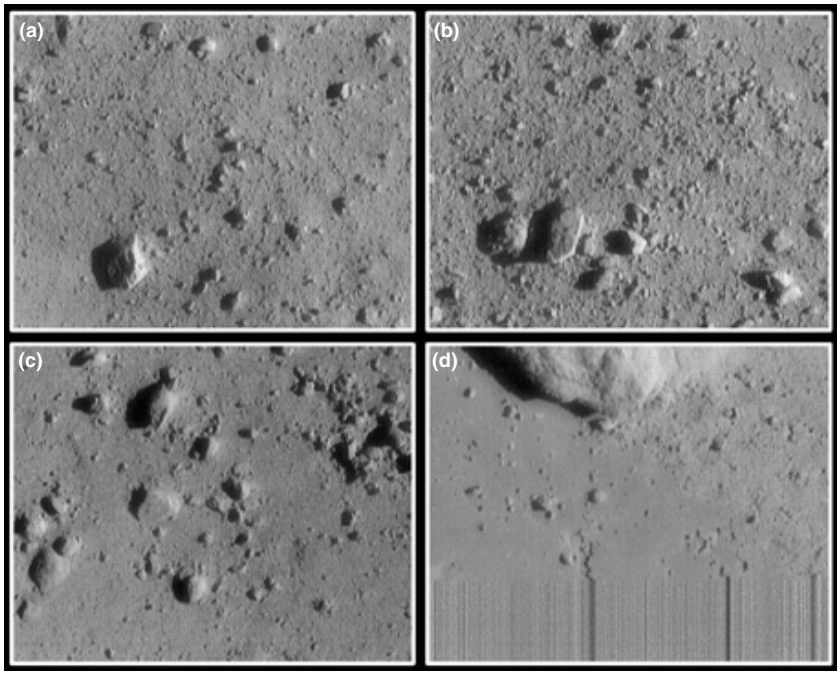

Figure 11. These four pictures are among the last ones taken by NEAR Shoemaker on 12 February 2001, during its successful descent to the surface of Eros. (a) Image was taken at about 1150 m from the surface and shows an area about 54 m wide. The large boulder rests upon the surface with some overhang, while some of the smaller boulders appear partly buried by finer loose material. (b) Image was taken from a range of 700 m and shows an area 33 m across. Small craters and cracks are visible in individual boulders. (c) Image was taken from a range of 250 m and shows an area only 12 m across. Different amounts of burial of the rocks and boulders are evident. (d) Last image was taken prior to touchdown from a range of 120 m and measures 6 m across. The bottom of the image was lost owing to interruption of its transmission to Earth as the spacecraft touched down. Part of a large boulder is visible at the top. At the bottom is a ponded deposit.

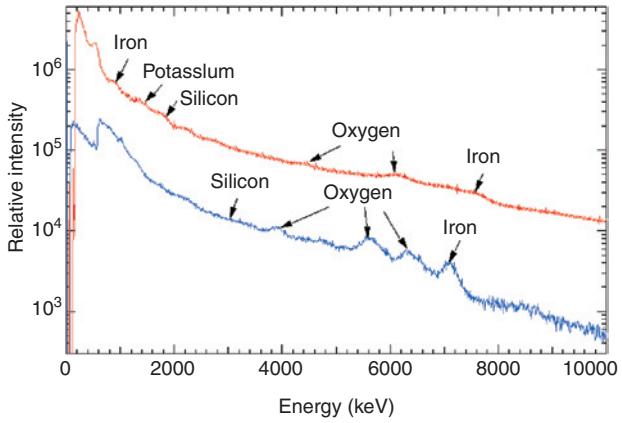

Figure 12. This graph displays the spectrum taken by the GRS from the surface of Eros following NEAR Shoemaker's historic landing. This spectrum is the result of 7 days of integrated measurements and is the first spectrum ever collected from the surface of an asteroid. The GRS consists of two detectors (the outer detector denoted in red and the inner detector in blue) which measure emitted light from the surface of the asteroid. The signatures of key elements are correlated to specific wavelengths of emission.

Multispectral Imager (MSI) clearly show a depletion of large particles in ponds,[56,66] implying that size sorting has occurred. The lack of evidence for Fe depletion in the XRS data, which cover more representative areas of the surface, along with the image observations, supports the interpretation that the Fe depletion is a pond characteristic.

Eros' silicate mineralogy (Fig. 13), as measured by the NIS, is consistent with ordinary chondrite meteorites.[44,51] The positions and relative depths of the observed pyroxene and olivine mineral absorptions are best correlated to L-, LL-, or H-type ordinary chondrites.[44,51] The visible and near-infrared spectra are inconsistent with known primitive achondrites.[69] The spatially resolved measurements revealed no convincing evidence for mineral compositional variation. The lack of spatial variation in the center of the 1-mm pyroxene/olivine absorption is evidence for compositional homogeneity on the order of hundreds of meters or larger.[44,51,62] The remarkable spectral uniformity of Eros may result from a uniformly high degree of space weathering from micrometeorite bombardment.[55]

The color observations obtained with the MSI, however, *do* show surprisingly large variations in albedo at 760 nm (Fig. 9), with the material being up to 1.5 times brighter than the average surface.[51,62,70] The depth of the 1-mm absorption (as opposed to the position of the center of the absorption) is several percent deeper for the bright materials than it is for the general surface.[51,62] Variations in the depth can be caused by differences in composition, particle size, or optical alteration due to space weathering. The inverse relationship between increased albedo and decreased absorption depth is characteristic of space weathering as observed on the Moon.[21,71,72] An older surface that has been exposed to the space environment for a longer period of time will have optical properties altered by the process of space weathering. Comparisons of the space weathering process on the Moon and Eros[62] suggest that the compositional difference between fresh materials on these two objects and/or differences in the microphysical processes of space weathering (such as those created by gravity or proximity to the Sun) significantly influence the optical characteristics of this process.

Significantly, no evidence for intrinsic magnetization of Eros[73] was observed, even during the descent to the surface. The absence of magnetization is consistent with a thermal history in which Eros was never heated to melting.

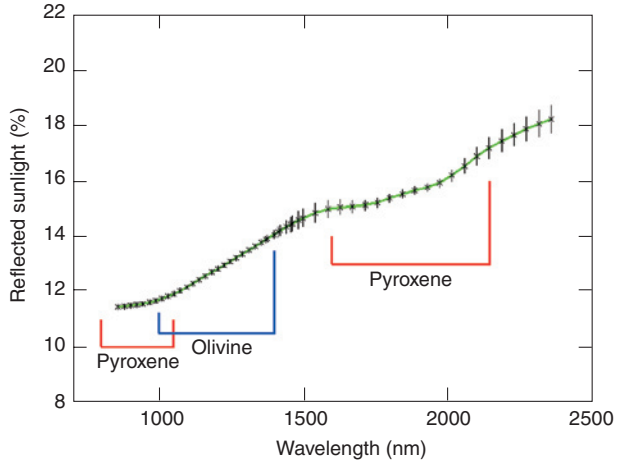

Figure 13. This graph displays a typical spectrum of Eros taken by the NIS prior to orbit insertion on 14 February 2000. The instrument measures the reflected sunlight reflected from the asteroid's surface over a wavelength range of 800–2400 nm. Absorption bands due to the rock-forming minerals olivine and pyroxene are seen in the 1000- and 2000-nm regions.

NEW QUESTIONS AND DIRECTIONS

The NEAR mission, a mission of many firsts in NASA's exploration program, substantially increased our understanding and knowledge of primitive bodies in our solar system. Although the data returned by NEAR have taught us many things about asteroids, much more remains to be learned. The questions answered have led to more intriguing, unanswered riddles.

The flyby of Mathilde provided a brief glimpse of only one face of this asteroid. However, for any plausible value of its volume, the density of Mathilde is low enough to imply a high porosity. Thus NEAR has demonstrated that large, highly porous, rubble pile asteroids do exist within the main belt. No new information was obtained on this asteroid's rotation state or the cause of its slow rotation. No compositional information was gleaned from this encounter. Many fascinating questions remain: Is its composition related to that of carbonaceous chondrites? What is the nature of

the porosity within Mathilde? What geologic structures (internal and external) have survived on this asteroid?

NEAR obtained much more detailed information during its orbital encounter with Eros. Images, laser altimetry, and radio science measurements have provided strong evidence for a consolidated, fractured asteroid with a regolith cover. The cohesive strength of bulk Eros was not usefully constrained. The presence of jointed and structurally controlled craters implies the presence of a substrate, with cohesive strength exceeding the gravitational stress, but the gravitational stress is very small on Eros. It is quite possible that the "consolidated substrate" of Eros may be weak enough to crumble easily in one's hand, or it may be much stronger. The geometric relations of grooves on Eros are suggestive of fractures in competent rock. The degree to which the interior has been fractured and the nature of the porosity have not been clearly constrained.

High-resolution imaging—down to a few centimeters per pixel—revealed a complex and active regolith, with many unexpected and puzzling features.[56] The paucity of craters smaller than 100 m in diameter and the profusion of blocks at tens of meters and below is one of the mysteries left by the NEAR observations. The variation in the depth of the regolith—from 100 m in some regions to near absence in others—is another. The processes forming the ponds, the debris aprons around some of the larger blocks, and the albedo contrasts are not well understood.

The spectral measurements also provided us with a new set of questions. While the spectral observations are consistent with an ordinary chondrite meteorite composition, the measurements did not establish an undisputed link between Eros and a specific meteorite class. Is Eros actually unrelated to any known meteorite type, or is it actually chondritic at depth, below the surface layers that may have been altered and fractionated by unknown weathering processes? The homogeneity observed in the spectral data contrasts with the stronger color variations seen in images of Ida and Gaspra.[44] On Ida, for example, relatively blue units (with a stronger 1-μm band) could be identified with fresh craters and even associated with ejecta from crater Azzura,[74] but no such phenomena were observed on Eros. It has been suggested that the different orbital histories of Ida and Eros are perhaps responsible for the variation,[55,62] but there is no conclusive evidence for this hypothesis.

One of the most surprising results obtained by NEAR at Eros was the lack of magnetization. Most meteorites, including chondrites, are much more strongly magnetized than Eros!

It will take many years before the wealth of data return by NEAR has been fully explored, but many of the outstanding questions may be resolved only by other missions. NEAR has shown that landed missions to asteroids are possible, and the information returned by *in situ* measurements, such as seismic sounding, or by sample return will answer many of the riddles NEAR has left for us and open the door to new discoveries about the early solar system.

REFERENCES

[1]Beatty, J. K., "NEAR Falls for Eros," *Sky and Telescope* **101**(5), 34–37 (2001).

[2]Farquhar, R., Veverka, J., and Williams, B., "Touchdown: NEAR's Hisoric Landing," *Planetary Report*, 6–11 (Sep–Oct 2001).

[3]Bottke, W. F., Rubincam, D., and Burns, J. "Dynamical Evolution of Main Belt Asteroids: Numerical Simulations Incorporating Planetary Perturbations and Yarkovsky Thermal Forces," *Icarus* **145**, 301–331 (2000).

[4]NEAR Science Working Group, *Near Earth Asteroid Rendezvous*, Report 86-7, JPL Laboratory, Pasadena, CA (1986).

[5]Binzel, R. P., Gaffey, M. J., Thomas, P. C., Zellner, B. H., Storrs, A. D., and Wells, E. N., "Geologic Mapping of Vesta from 1994 Hubble Space Telescope Images," *Icarus* **128**, 95–103 (1997).

[6]Zellner, B. H., Albrecht, R., Binzel, R. P., Gaffey, M. J., Thomas, P. C., et al., "Hubble Space Telescope Images of Asteroid 4 Vesta in 1994," *Icarus* **128**, 83–87 (1997).

[7]Lebofsky, L. A., McCarthy, D., Hege, E. K., Binzel, R. P., Drummond, J., et al., "Mineralogic Mapping of Asteroid 4 Vesta from 1–2 microns with NICMOS/HST," *BAAS* **30**, 07.P09. (1998).

[8]Carvano, J. M., Mccarthy, D. W., Binzel, R., Drummond, J., Gaffey, M., et al., "Mineralogical Mapping of Asteroid 4 Vesta with HST/NICMOS: First Results," *BAAS* **32**, 08.05 (2000).

[9]Storrs, A. D., Makhoul, K., Gaffey, M. J., Landis, R., Vilas, F., et al., "Initial Analysis of HST Snapshot Images of Asteroids," *BAAS* **33**, 41.14 (2001).

[10]Storrs, A., Wells, E., Zellner, B., Stern, A., and Durda, D., "Imaging Observations of Asteroids with HST," *BAAS* **31**, 11.03 (1999).

[11]Storrs, A., Wells, E., Stern, A., and Zellner, B., "Surface Heterogeneity of Asteroids: HST WFPC2 Images 1996–1997," *BAAS* **30**, 07.P12 (1998).

[12]Parker, J. W., Stern, S. A., Merline, W. J., Festou, M. C., Thomas, P. C., et al., "HST/FOC Observations of Ceres," *BAAS* **30**, 05.02 (1998).

[13]Parker, J. W., Stern, S. A., Thomas, P. C., Festou, M. C., Merline, W. J., et al., "Analysis of the First Disk-Resolved Images of Ceres from Ultraviolet Observations with the Hubble Space Telescope," *BAAS* **33**, 41.15 (2001).

[14]Thomas, P. C., Veverka, J., Simonelli, D., Helfenstein, P., Carcich, B., et al., "The Shape of Gaspra," *Icarus* **107**, 23–36 (1994).

[15]Davis, D. R., Ryan, E., and Farinella, P., "Asteroid Collisional Evolution: Results from Current Scaling Algorithms," *Planet. Space Sci.* **42**, 599–610 (1994).

[16]Melosh, H., and Ryan, E., "Asteroids: Shattered But Not Dispersed," *Icarus* **129**, 562–564 (1997).

[17]Ostro, S., Pravec, P., Benner, L., Hudson, S., Sarounova, L., et al., "Radar and Optical Observations of Asteroid 1998 KY26," *Science* **285**, 557–559 (1999).

[18]Pravec, P., and Harris, A. W., "Asteroid Rotations," in *Proc. Asteroids 2001 Conf.* (2001).

[19]Gaffey, M. J., Burbine, T. H., and Binze, R. P., "Asteroid Spectroscopy: Progress and Perspectives," *Meteoritics* **28**, 161–187 (1993).

[20]Chapman, C. R., "S-type Asteroids, Ordinary Chondrites, and Space Weathering: The Evidence from Galileo's Fly-bys of Gaspra and Ida," *Meteorit. Planet. Sci.* **31**, 699–725 (1996).

[21]Hapke, B., "Space Weathering from Mercury to the Asteroid Belt," *J. Geophys. Res.* **106**, 10,039–10,073 (2001).

[22]Belton, M. J. S., Veverka, J., Thomas, P., Helfenstein, P., Simonelli, D., et al., "Galileo Encounter with 951 Gaspra: First Pictures of an Asteroid," *Science* **257**, 1647–1652 (1992).

[23]Belton, M. J. S., Chapman, C. R., Veverka, J., Klaasen, K. P., Harch, A., et al., "First Images of 243 Ida," *Science* **265**, 1543–1547 (1994).

[24]Belton, M. J. S., Mueller, B. E. A., D'Amario, L. A., Byrnes, D. V., Klaasen, K. P., et al., "The Discovery and Orbit of 1993 (243)1 Dactyl," *Icarus* **120**, 185–199 (1996).

[25]Veverka, J., Thomas, P., Harch, A., Clark, B., Bell III, J. F., et al., "NEAR's Flyby of 253 Mathilde: Images of a C Asteroid," *Science* **278**, 2109–2114 (1997).

[26]Yeomans, D., Barriot, J-P., Dunham, D. W., Farquhar, R. W., Giogini, J. D., et al., "Estimating the Mass of Asteroid 253 Mathilde from Tracking Data During the NEAR Flyby," *Science* **278**, 2106–2109 (1997).
[27]Mottola S. W., Sears, D., Erikson, A., Harris, A. W., Young, J. W., et al., "The Slow Rotation of 253 Mathilde," *Planet. Space Sci.* **43**, 1609–1613 (1995).
[28]Hiroi, T., Pieters, C. M., Zolensky, M. E., and Lipschutz, M. E., "Evidence of Thermal Metamorphism on the C, G, B, and F Asteroids," *Science* **261**, 1016–1018 (1993).
[29]Binzel, R. P., Burbine, T. H., and Bus, S. J., "Groundbased Reconnaissance of Asteroid 253 Mathilde: Visible Wavelength Spectrum and Meteorite Comparison," *Icarus* **119**, 447–449 (1996).
[30]Veverka, J., Thomas, P., Harch, A., Clark, B., Bell III, J. F., et al., "NEAR Encounter with Asteroid 253 Mathilde: Overview," *Icarus* **140**, 3–16 (1999).
[31]Chapman, C. R., Merline, W. J., and Thomas, P., "Cratering on Mathilde," *Icarus* **140**, 28–33 (1999).
[32]Thomas, P. C., Veverka, J., Bell III, J. F., Clark, B. E., Carcich, B., et al., "Mathilde: Size, Shape, and Geology," *Icarus* **140**, 17–27 (1999).
[33]Housen, K. R., Holsapple, K. A., and Voss, M. E., "Compaction as the Origin of the Unusual Craters on the Asteroid Mathilde," *Nature* **402**, 155–157 (1999).
[34]Housen, K. R., Schmidt, R. M., and Holsapple, K. A., "Crater Ejecta Scaling Laws: Fundamental Forms Based on Dimensional Analysis," *J. Geophys. Res.* **88**, 2485–2499 (1983).
[35]Greenberg, R., Nolan, M. C., Bottke, W. F., and Kolvoord, R. A., "Collisional History of Gaspra," *Icarus* **107**, 84–97 (1994).
[36]Greenberg, R., Bottke, W. F., Nolan, M., Geissler, P., Petit, J.-M., and Durda, D. D., "Collisional and Dynamical History of Ida," *Icarus* **120**, 106–118 (1996).
[37]Asphaug, E., Moore, J. M., Morrison, D., Benz, W., Nolan, M. C., and Sullivan R., "Mechanical and Geological Effects of Impact Cratering on Ida," *Icarus* **120**, 158–184 (1996).
[38]Cheng, A. F., and Barnouin-Jha, O. S., "Giant Craters on Mathilde," *Icarus* **140**, 34–48 (1999).
[39]Clark, B. E., Veverka, J., Helfenstein, P., Thomas, P. C., Bell III, J. F., et al., "NEAR Photometry of Asteroid 253 Mathilde," *Icarus* **140**, 53–65 (1999).
[40]Murchie, S., Domingue, D., Robinson, M., Li, H., Prockter, L., et al., "Inflight Calibration of the NEAR Multispectral Imager, 2: Results at Eros," *Icarus* **155**, 229–243 (2002).
[41]Yeomans, D. K., Antreasian, P. G., Barriot, J.-P., Chesley, S. R., Dunham, D. W., et al., "Radio Science Results During the NEAR-Shoemaker Spacecraft Rendezvous with Eros," *Science* **289**, 2085–2088 (2000).
[42]Zellner, B., "Physical Properties of Asteroid 433 Eros," *Icarus* **28**, 149–153 (1976).
[43]Mitchell, D. L., Hudson, R. S., Ostro, S. J., and Rosema, K. D., "Shape of Asteroid 433 Eros from Inversion of Goldstone Radar Doppler Spectra," *Icarus* **131**, 4–14 (1998).
[44]Veverka, J., Robinson, M., Thomas, P., Murchie, S., Bell III, J. F., et al., "NEAR at Eros: Imaging and Spectral Results," *Science* **289**, 2088–2097 (2000).
[45]Zuber, M. T., Smith, D. E., Cheng, A. F., Garvin, J. B., Aharonson, O., et al., "The Shape of 433 Eros from the NEAR-Shoemaker Laser Rangefinder," *Science* **289**, 2097–2101 (2000).
[46]Wilkison, S. L., and Robinson, M. S., "Bulk Density of Ordinary Chondrite Meteorites and Implications for Asteroidal Internal Structure," *Meteorit. Planet. Sci.* **35**, 1203–1213 (2000).
[47]Wilkison, S. L., Robinson, M. S., Thomas, P. C., Veverka, J., McCoy, T. J., et al., "An Estimate of Eros's Porosity and Implications for Internal Structure," *Icarus* **155**, 94–103 (2002).
[48]Sullivan, R., Thomas, P., Murchie, S., and Robinson, M., *Asteroid Geology from Galileo and NEAR Data. Asteroids III*, University of Arizona Press (2002).
[49]Miller, J. K., Konopliv, A. S., Antreasian, P. G., Bordi, J. J., Chesley S., et al., "Determination of Shape, Gravity and Rotational State of Asteroid 433 Eros," *Icarus* **155**, 3–17 (2002).
[50]Thomas, P. C., Robinson, M. S., Veverka, J., and Murchie, S., "Shoemaker Crater as a Major Source of Ejecta on Asteroid 433 Eros," *Nature* **413**, 394–396 (2001).
[51]Bell III, J. F., Izenberg, N. I., Lucey, P. G., Clark, B. E., P.son, C., et al., "Near-IR Reflectance Spectroscopy of 433 Eros from the NIS Instrument on the NEAR Mission. 1. Low Phase Angle Observations," *Icarus* **155**, 119–140 (2002).
[52]Trombka, J., Squyres, S., Brückner, J., Boynton, W., Reedy, R., et al., "The Elemental Composition of Asteroid 433 Eros: Results of the NEAR-Shoemaker X-Ray Spectrometer," *Science* **289**, 2101–2105 (2000).
[53]Prockter, L., Thomas, P., Robinson, M., Joseph, J., Milne, A., et al., "Surface Expressions of Structural Features on Eros," *Icarus* **155**, 75–93 (2002).
[54]Thomas, P. C., Joseph, J., Carcich, B., Veverka, J., Clark, B. E., et al., "Eros: Shape, Topography, and Slope Processes," *Icarus* **155**, 18–37 (2002).
[55]Chapman, C. R., Merline, W. J., Thomas, P. C., Joseph, J., Cheng, A. F., and Izenberg, N., "Impact History of Eros: Craters and Boulders," *Icarus* **155**, 104–118 (2002).
[56]Veverka, J., Thomas, P. C., Robinson, M., Murchie, S., Chapman, C., et al., "Imaging of Small-Scale Features on 433 Eros from NEAR: Evidence for a Complex Regolith," *Science* **292**, 484–488 (2001).
[57]Zellner, B., and Gradie, J., "Polarization of the Reflected Light of Asteroid 433 Eros," *Icarus* **28**, 117–123 (1976).
[58]Morrison, D., "The Diameter and Thermal Inertia of 433 Eros," *Icarus* **28**, 125–132 (1976).
[59]Lebofsky, L. A., and Rieke, G. H., "Thermal Properties of 433 Eros," *Icarus* **40**, 297–308 (1979).
[60]Cheng, A. F., Barnouin-Jha, O., Prockter, L., Zuber, M., Neumann, G., et al., "Small Scale Topography of 433 Eros from Laser Altimetry and Imaging," *Icarus* **155**, 51–74 (2002).
[61]Barnouin-Jha, O. S., Garvin, J. B., Cheng, A. F., Zuber, M., Smith, D., et al., "Preliminary Impact Crater Dimensions on 433 Eros from the NEAR Laser Range-Finder and Imager," in *Lunar and Planetary Science XXXII*, Abstract #1786, Lunar and Planetary Institute, Houston, TX (CD-ROM) (2001).
[62]Murchie, S., Robinson, M., Clark, B., Li, H., Thomas, P., et al., "Color Variations on Eros from NEAR Multispectral Imaging," *Icarus* **155**, 145–168 (2002).
[63]Clark, B. E., Helfenstein, P., Bell, J. F., Peterson, C., Veverka, J., et al., "NEAR Infrared Spectrometer Photometry of Asteroid 433 Eros," *Icarus* **155**, 189–204 (2002).
[64]Veverka, J., Farquhar, B., Robinson, M., Thomas, P., Murchie, S., et al., "The landing of the NEAR-Shoemaker Spacecraft on Asteroid 433 Eros," *Nature* **13**, 390–393 (2001).
[65]Cheng, A. F., Barnouin-Jha, O., Zuber, M., Veverka, J., Smith, D. E., et al., "Laser Altimetry of Small-Scale Features on 433 Eros from NEAR Shoemaker," *Science* **292**, 488–491 (2001).
[66]Robinson, M. S., Thomas, P. C., Veverka, J., Murchie, S., and Carcich, B. T., "Morphology, Distribution and Origin of Ponded Deposits on Eros," *Nature* **413**, 396–400 (2001).
[67]Evans, L. G., Starr, R. D., Bruckner, J., Reedy, R. C., Boynton, W. V., et al., "Elemental Composition from Gamma-Ray Spectroscopy of the NEAR-Shoemaker Landing Site on 433 Eros," *MAPS* **36**(12), 1639–1660 (2002).
[68]Evans, L., Starr, R., Brückner, J., Reedy, R., Boynton, W., et al., "Elemental Composition from Gamma-Ray Spectroscopy of the NEAR-Shoemaker Landing Site on 433 Eros," *Meteorit. Planet. Sci.* **36**, 1639–1660 (2001).
[69]Burbine, T. H., McCoy, T. J., Nittler, L. R., and Bell III, J. F., "Could 433 Eros Have a Primitive Achondritic Composition?" in *Lunar and Planet. Sci. XXXII*, Abstract #1860, LPI, Houston (CD-ROM) (2001).
[70]Clark, B. E., Lucey, P. G., Helfenstein, P., Bell III, J. F., P.son C., et al., "Space Weathering on Eros: Constraints from Albedo and Spectral Measurements of Psyche Crater," *Meteorit. Planet. Sci.* **36**, 1617–1638 (2001).
[71]Adams, J. B., and McCord, T. M., "Alteration of Lunar Optical Properties: Age and Composition Effects," *Science* **171**, 4829–4836 (1971).
[72]Pieters C. M., Taylor, L. A., Noble, S. K., Keller, L. P., Hapke B., et al., "Space Weathering on Airless Bodies: Resolving a Mystery with Lunar Samples," *Meteorit. Planet. Sci.* **35**, 1101–1107 (2000).
[73]Acuña, M. H., Anderson, B. J., Russell, C. T., Wasilewski, P., Kletetshka, G., et al., "NEAR Magnetic Field Observations at 433 Eros: First Measurements from the Surface of an Asteroid, *Icarus* **155**, 220–228 (2002).
[74]Geissler, P., Petit, J-M., Durda, D. D., Greenberg, R., Bottke, W., Nolan, M., and Moore, J., "Erosion and Ejecta Reaccretion on 243 Ida and Its Moon," *Icarus* **120**, 140–157(1996).

THE AUTHORS

DEBORAH L. DOMINGUE received a B.S. in physics from the University of Vermont in 1985 and a Ph.D. in geology and planetary sciences from the University of Pittsburgh in 1990. She joined APL in 1997. Dr. Domingue's research interests include the study of planetary surface properties from objects as diverse as asteroids to the icy surfaces of the outer planet satellites. She was as associate member of the NEAR imaging/spectroscopy science team and is currently the deputy project scientist for the MESSENGER mission to Mercury. Her e-mail address is deborah.domingue@jhuapl.edu.

ANDREW F. CHENG received an A.B. in physics from Princeton University in 1971 and a Ph.D. in physics from Columbia University in 1977. He joined APL in 1983. Dr. Cheng's research interests include the physics of asteroids and the magnetospheres of the outer planets. He was the project scientist for the highly successful NEAR mission and is currently the project scientist for the New Horizons mission to Pluto. He is an interdisciplinary scientist for the Galileo mission, a co-investigator for the MIMI instrument on the Cassini mission, the Orbiter LIDAR scientist for the MUSES-C mission, and a science team member on the MESSENGER mission to Mercury. Dr. Cheng has served as an associate editor of the *Journal of Geophysical Research* and *Geophysical Research Letters* and as editor (for Solar-Planetary Relations) of *EoS: Transactions of the American Geophysical Union*. His e-mail address is andrew.cheng@jhuapl.edu.